Astronomy & Astrophysics manuscript no. Hincelin
October 30, 2014
©ESO 2014

A new and simple approach to determine the abundance of hydrogen molecules on interstellar ice mantles

U. Hincelin[1], Q. Chang[2, 3], and E. Herbst[1]

[1] Department of Chemistry, University of Virginia, Charlottesville, VA 22904, USA
e-mail: ugo.hincelin@virginia.edu
[2] XinJiang Astronomical Observatory, Chinese Academy of Sciences, 150 Science 1-Street, Urumqi 830011, PR China
[3] Key Laboratory of Radio Astronomy, Chinese Academy of Sciences, 2 West Beijing Road, Nanjing 210008, PR China

October 30, 2014

arXiv:1410.7375v2 [astro-ph.SR] 29 Oct 2014

ABSTRACT

Context. Water is usually the main component of ice mantles, which cover the cores of dust grains in cold portions of dense interstellar clouds. When molecular hydrogen is adsorbed onto an icy mantle through physisorption, a common assumption in gas-grain rate-equation models is to use an adsorption energy for molecular hydrogen on a pure water substrate. However, at high density and low temperature, when H_2 is efficiently adsorbed onto the mantle, its surface abundance can be strongly overestimated if this assumption is still used. Unfortunately, the more detailed microscopic Monte Carlo treatment cannot be used to study the abundance of H_2 in ice mantles if a full gas-grain network is utilized.

Aims. We present a numerical method adapted for rate-equation models that takes into account the possibility that an H_2 molecule can, while diffusing on the surface, find itself bound to another hydrogen molecule, with a far weaker bond than the H_2-water bond, which can lead to more efficient desorption. We label the ensuing desorption "encounter desorption".

Methods. The method is implemented first in a simple system consisting only of hydrogen molecules at steady state between gas and dust using the rate-equation approach and comparing the results with the results of a microscopic Monte Carlo calculation. We then discuss the use of the rate-equation approach with encounter desorption embedded in a complete gas-grain chemical network.

Results. For the simple system, the rate-equation model with encounter desorption reproduces the H_2 granular coverage computed by the microscopic Monte Carlo model at 10 K for a gas density from 10^4 to 10^{12} cm^{-3}, and yields up to a factor 4 difference above 10^{12} cm^{-3}. The H_2 granular coverage is also reproduced by a complete gas-grain network. We use the rate-equation approach to study the gas-grain chemistry of cold dense regions with and without the encounter desorption mechanism. We find that the grain surface and gas phase species can be sensitive to the H_2 coverage, up to several orders of magnitude, depending on the species, the density, and the time considered.

Conclusions. The method is especially useful for dense and cold environments, and for time-dependent physical conditions, such as occur in the collapse of dense cores and the formation of protoplanetary disks. It is not significantly CPU time consuming, so can be used for example with complex 3D chemical-hydrodynamical simulations.

Key words. astrochemistry – molecular processes – methods: numerical – ISM: molecules – ISM: abundances

1. Introduction

Gas-grain chemical models, which are useful tools for studying the chemistry in the interstellar medium, often include the rate-equation approach to calculate the evolution of species in the gas phase and on the grain surface (e.g., Herbst & Klemperer 1973; Hasegawa et al. 1992). Regarding the chemistry on dust grains and their ice mantles, the rate-equation approach can be used in the basic two-phase approach, in which no distinction is made between the surface of the ice and layers underneath it, the three-phase model, in which chemistry only takes place on the surface, or even a multi-layer approach (e.g., Hasegawa et al. 1992; Hasegawa & Herbst 1993b; Taquet et al. 2012). Even the two-phase approach can describe the chemistry reasonably accurately (Garrod et al. 2008), and rate-equation methods are efficient for large chemical networks where thousands of reactions are taken into account. Some limitation exists when the average number of species per dust grain is below unity, and stochastic methods are more accurate (Tielens & Charnley 1997; Caselli et al. 1998; Herbst & Shematovich 2003; Lipshtat & Biham 2003; Stantcheva & Herbst 2004). Contrary to microscopic kinetic Monte Carlo models, and other detailed stochastic treatments, (Chang et al. 2005; Cuppen & Herbst 2005; Chang et al. 2007; Cuppen et al. 2009; Cazaux et al. 2010; Chang & Herbst 2012; Iqbal et al. 2012; Chang & Herbst 2014), rate-equation models do not take into account each individual process that occurs on and beneath the ice surface. For example, when a molecule is adsorbed on the grain surface, the desorption energy should depend on the substrate and other grain surface parameters, which are functions of the location on the grain surface, itself continuously in evolution as a function of time. For rate-equation treatments, however, a single binding energy per adsorbate is commonly used depending upon physical conditions and type of source. Since water ice is often the main component of dust grain mantles in cold dense interstellar clouds (Tielens & Hagen 1982; Whittet et al. 1998), the adsorption energies used in models of these sources are usually the ones of a given adsorbate on a water substrate. A list of desorption energies for a selection of physisorbed adsorbates on water and other substrates can be found in Table 3 of Cuppen & Herbst (2007). In this paper we will be concerned with the binding of H_2 on a water substrate

and on itself, and will be using 440 K and 23 K on H_2 for the two values, respectively (Cuppen & Herbst 2007).

Determination of the amount of H_2 on a dust grain in a cold cloud is a difficult task for several reasons. First, it is difficult if not impossible to include the adsorption and desorption of hydrogen molecules in a complete treatment of the surface chemistry via the kinetic Monte Carlo approach given the speed with which these events can happen. The situation gets worse if complex simulations of star formation, such as three-dimensional hydrodynamical simulations (Furuya et al. 2012; Hincelin et al. 2013), or even warm-up models (e.g. Viti et al. 2004; Garrod & Herbst 2006), are undertaken, because the kinetic Monte Carlo models are very time-consuming computationally. Secondly, the large difference between the binding energy of H_2 to a water ice substrate and to itself means that a rate-equation model with only one binding energy for H_2, the one with water, can lead to an overestimate of the H_2 granular abundance, especially at low temperature and high density (≈10 K and $>10^4$ cm^{-3}), and on the contrary, considering a single binding energy of 23 K prevents adsorption of H_2 onto grain surfaces, which is not real except at high temperatures. Thus, a simple and efficient numerical approach to deal with H_2 coverage as a function of temperature, density, and time, and applicable to rate-equation chemical models, is desirable. The goal of this paper is to present one such approach and to use it in treatments of cold and dense regions. This new approach differs from earlier approaches of Wolff et al. (2010), Cuppen & Garrod (2011), and Garrod & Pauly (2011).

The remainder of the paper is structured as follows. We present our treatment in terms of a rate equation in Section 2. In Section 3, we then consider a simple steady-state model in which we only include a fixed amount of H_2 and calculate the surface abundance of H_2 as a function of density for a cloud at 10 K. We compare the results of this simple model with those of a detailed kinetic Monte Carlo approach. The two approaches lead to very similar results for the H_2 surface abundance. In Section 4, we introduce a large gas-grain network and code with encounter desorption, based on the Nautilus model (Hersant et al. 2009), and use it to obtain the H_2 surface abundance as a function of density. The good agreement with the simple treatments suggests that we can use a large gas-grain rate-equation treatment with encounter desorption to determine the overall chemistry that occurs as a function of H_2 surface abundance. The chemistry is discussed in Section 5, and a conclusion follows.

2. The "encounter desorption" mechanism

Water is the main component of the ice mantle, therefore the desorption energy of a species on a water substrate is usually used. However, at very high density, H_2 can become quite abundant on the grain surface, since it is the most abundant species in the gas phase. In an extreme case, we would need to use the binding energy of adsorbates to H_2 and not to water (Morata & Hasegawa 2013). To take this problem into account, Garrod & Pauly (2011) calculated effective binding energies and diffusion barriers according to the fractional coverage of the surface with H_2. This method produces a maximum H_2-ice fraction of around 10 % under cold molecular cloud conditions. Unfortunately, desorption energies and diffusion barriers of every species become time dependent using this technique. Then the differential equation system become stiffer than usual and as a consequence more difficult to solve, which could be a handicap for complex hydrodynamical simulations (Furuya et al. 2012; Hincelin et al. 2013), where computing time is a critical limitation.

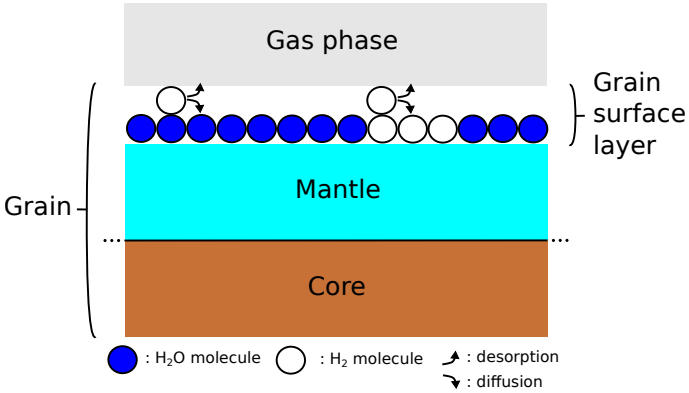

Fig. 1. An interstellar grain covered by a mantle of ice. The surface layer is composed of water and molecular hydrogen, and H_2 molecules diffuse on the surface.

Our approach, which we label "encounter" desorption, is a different one. Figure 1 shows an interstellar grain consisting of a silicate or carbonaceous core, and an ice mantle assumed mainly to be of water ice, with water molecules in the top layer illustrated in dark blue, and hydrogen molecules in white. Individual hydrogen molecules diffuse for the most part over water molecules until they reach another hydrogen molecule beneath them, at which time the binding energy of the diffusing species is sharply reduced from 440 K to 23 K, raising the likelihood of desorption. The desorption of an H_2 molecule due to the lower desorption energy, when the molecule ends up on an H_2 substrate, is modeled by considering the encounter of two H_2 molecules on the same surface site. The grain surface "reaction" H_2(grain) + H_2(grain) $\longrightarrow$ H_2(grain) + H_2(gas) is added to the reaction network with a specific reaction rate $R_{H_2H_2}$ to take into account this process.

The rate is given by

$$R_{H_2H_2} = \frac{1}{2} k_{H_2H_2} n_s(H_2) n_s(H_2) \kappa(H_2), \quad (1)$$

in units of cm^{-3} s^{-1}, where $k_{H_2H_2}$ is the rate coefficient (cm^3 s^{-1}) at which two hydrogen molecules diffuse into the same lattice site (Hasegawa et al. 1992; Caselli et al. 1998), the hydrogen concentration on grain surfaces is written as $n_s(H_2)$ (cm^{-3}) and $\kappa(H_2)$ is the probability of desorption rather than diffusion. This probability is given by the equation

$$\kappa(H_2) = \frac{\sum_X k_{Xdes}(H_2)}{R_{diff}(H_2) + \sum_X k_{Xdes}(H_2)} \quad (2)$$

where the sum over X is a sum over the thermal desorption rate coefficient and assorted non-thermal desorption rate coefficients (s^{-1}) due to photons and cosmic rays. In the general case, we take into account thermal desorption, cosmic ray induced desorption, and photodesorption from direct interstellar UV photons and secondary photons generated by cosmic rays (see Hasegawa et al. 1992; Hasegawa & Herbst 1993a; Leger et al. 1985; Öberg et al. 2007, 2009a,b,c; Hassel et al. 2008, 2010)), while R_{diff} is the diffusion rate (s^{-1}) of one H_2 molecule on an H_2 substrate (Hasegawa et al. 1992; Caselli et al. 1998).

3. A comparison between different methods for a simple system

Before we apply our encounter desorption mechanism to a realistic gas-grain simulation, the validity of the mechanism has to be tested. Since the microscopic Monte Carlo approach is the most rigorous simulation method, ideally we should compare the results of the rate equation approach including encounter desorption with analogous results with the microscopic Monte Carlo simulation results using a full reaction network. However, since the gas phase H_2 abundance is too large to be treated by the Monte Carlo method, we choose a system that is as simple as possible. In this section, we report the results of a comparative study of such a simple system, in which we consider only H_2 and a mantle of effectively water ice. We then compute the steady-state fraction of molecular hydrogen on the dust grains at 10 K as a function of total H_2 density. We take a typical grain with radius 0.1μm and 10^6 binding sites, and a gas-to-dust number density of 10^{-12}. H_2 from the gas can accrete onto a grain surface and then diffuse or desorb from the surface. Thermal desorption is treated in the standard manner, while the rate coefficient for encounter desorption is treated as in equation (1), but without non-thermal desorption mechanisms.

The simple rate equation approach is based on setting the time derivative of the concentration of H_2 on grains to zero:

$$\frac{d\, n_s(H_2)}{dt} = k_{ads}(H_2) n_g(H_2) - R_{H_2H_2} - k_{\theta des}(H_2) n_s(H_2) = 0 \quad (3)$$

and solving for the H_2 grain concentration. In the equation, $n_g(H_2)$ is the gas-phase H_2 abundance, k_{ads} is the adsorption rate coefficient for H_2, $k_{\theta des}$ is its thermal desorption rate coefficient (Hasegawa et al. 1992), and the rate for encounter desorption is to be found in equation (1).

The microscopic Monte Carlo simulation method has been explained in detail in Chang et al. (2005), so will only be discussed briefly here. A grain surface with N binding sites is represented as an $L \times L$ square lattice, where L is the number of sites on grain surface in one dimension. We keep track of the position and movement of H_2 species on the lattice. The movements, which include hopping, desorption, and adsorption, are modeled as Poisson processes, so that the time interval between two successive movement operations, Δt, is given by

$$\Delta t = \frac{\ln(x)}{k}, \quad (4)$$

where x is a random number uniformly distributed within 0 and 1, and k (in s^{-1}) is the hopping rate coefficient k_{hop}, the thermal desorption rate coefficient $k_{\theta des}$, or the adsorption rate coefficient k_{ads}, depending on the specific movement operation. Moreover, hopping will compete with desorption for an H_2 species that resides in a binding site. We combine hopping and desorption as a joint Poisson process and then use a competition mechanism to decide whether the species will hop or desorb (Chang et al. 2005).

Figure 2 shows the steady-state molecular hydrogen abundance on a grain surface, calculated as a function of H_2 total density (gas and grain surface) for three models, two of which contain no encounter desorption using a desorption energy for H_2 of either 440 K, the H_2-water value, or 23 K, the H_2-H_2 value. For these models, only the rate-equation result is shown. The third model contains the encounter desorption rate process as well as thermal desorption using the 440 K desorption energy,

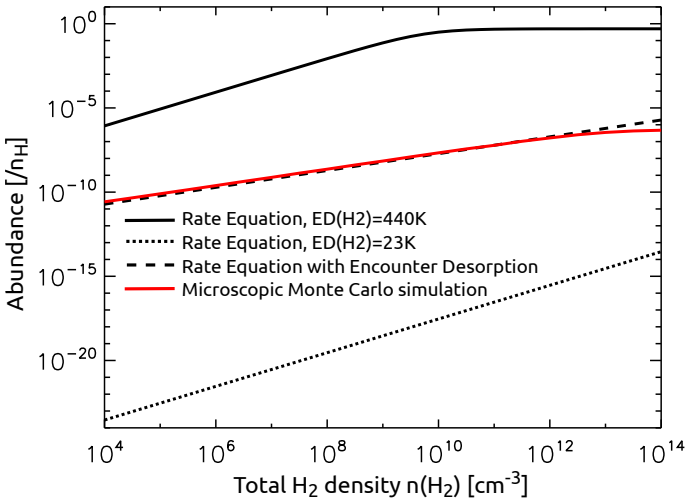

Fig. 2. H_2 fractional abundance on the dust surface with respect to the total proton abundance plotted against the total (gas and grain surface) hydrogen density, as computed by different methods for a simple system at steady state (see text in Section 3).

which is a very slow process at 10 K[1]. For this case, we also plot the result of the kinetic Monte Carlo approach, which should reproduce the H_2 granular abundance of the encounter desorption rate-equation model if the latter is accurate. Note that the kinetic Monte Carlo model assumes a constant gas phase H_2 abundance, which is not the case using the rate-equation approach. The grain surface abundance of H_2 is, however, very small compared with the gas phase H_2 using the Monte Carlo model, so this assumption does not change our results presented in the figure.

Both models without encounter desorption show a linear dependence of the H_2 surface abundance on total proton density n_H for at least a portion of the H_2 densities considered. With the higher desorption energy, H_2 is slowly desorbed, so that as the H_2 density approaches 10^{11} cm^{-3}, virtually all molecular hydrogen is located on grains, reaching a fractional abundance of 0.5 with respect to the total proton density. With the lower desorption energy, the average number of H_2 molecules per grain is less than unity even at the highest density utilized (abundance $\approx 10^{-14} - 10^{-13}$). With encounter desorption, the results lie in-between, with the H_2 granular fractional abundance at a standard dense cloud gas density of 10^4 cm^{-3} approximately 10^{-9}, which corresponds to about 40 molecules per grain, and, at the highest density studied, 4×10^6 molecules per grain, which corresponds to $\sim$ 4 monolayers. The surface fractional abundance calculated with the rate equation model including encounter desorption is slightly larger than the value obtained with the microscopic Monte Carlo model at densities larger than 10^{12} cm^{-3}, because in the rate-equation model, the H_2 grain surface concentration is approximately linearly dependent on the density of the medium, whereas the Monte Carlo model involves one monolayer of H_2 as a limit. However, even at the highest density in our simulation, 10^{14} cm^{-3}, the encounter desorption model result for the grain H_2 abundance is only about a factor of 4 larger than the microscopic Monte Carlo model value.

[1] In this third model, 440 K is used in the rate coefficient $k_{H_2H_2}$ in equation 1, while 23 K is used in the different terms of the probability $\kappa(H_2)$ shown in equation 2.

4. Results with encounter desorption and a large gas-grain reaction network

Given the degree of agreement between the kinetic Monte Carlo method and the encounter desorption rate-equation method for a simple system, we have chosen to extend the encounter desorption approach to a full gas-grain model, using the Nautilus code (Hersant et al. 2009). The two-phase rate-equation approach is used, in which no distinction is made between the inner and surface layers of the mantle. Details on the processes included in the code are presented by Semenov et al. (2010) and Hincelin (2012). The potential energy barrier against diffusion, E_b, is linked to the desorption energy E_D by the equation $E_b = \alpha E_D$. We set α equal to 0.5 as in Garrod & Herbst (2006), although other estimates exist, typically ranging from 0.3 to 0.77 (Watson 1976; Tielens & Allamandola 1987; Hasegawa et al. 1992; Ruffle & Herbst 2000). We used the chemical network of Hincelin et al. (2013), which includes the latest recommendations from the KIDA experts on gas-phase processes until October 2011. An electronic version of this network is available at `http://kida.obs.u-bordeaux1.fr/models`. Photodesorption has been included following Öberg et al. (2007, 2009a,b,c) and Hassel et al. (2008, 2010) and a limiting factor is added to restrict the mechanism to two monolayers. Two sources of incident UV radiation are considered : direct interstellar UV photons, and secondary photons generated by cosmic rays. We used the elemental abundances following Hincelin et al. (2011)[2] with an oxygen elemental abundance relative to hydrogen of 3.3×10^{-4}. The species are assumed to be initially in an atomic form as in diffuse clouds except for hydrogen, which is initially in H_2 form. Elements with an ionization potential below 13.6 eV – C, S, Si, Fe, Na, Mg, Cl, and P – are initially singly ionized. From the initial state, the chemistry evolves under cold and dense conditions. The gas and grain temperature are equal to 10 K, the cosmic-ray ionization rate is 1.3×10^{-17} s^{-1}, and the visual extinction is set to 30. The density is once again varied in the range $\sim 10^4$ cm^{-3} to $\sim 10^{14}$ cm^{-3}. We have run three different models, summarized in Table 1, which are analogous to those used for the simple models. In models 440-noED and 23-noED, the desorption energy of H_2 is fixed to 440 K and 23 K, respectively, and the encounter desorption mechanism is disabled. In model 440-ED, the desorption energy of H_2 is fixed to 440 K and the encounter desorption mechanism is enabled with a desorption energy equal to 23 K.

Table 1. Model designations for full gas-grain simulation

Model	H_2 Desorption Energy	Encounter Desorption
440-noED	440 K	disabled
23-noED	23 K	disabled
440-ED	440 K	enabled

Figure 3 shows the abundance of H_2 at steady state in the gas phase and on a grain surface for all three models, as a function of total gaseous plus surface hydrogen density. Steady state for H_2 is reached before 10 yr since its high abundance in the gas phase causes a high adsorption rate, and because we start with all hydrogen in its molecular form. The steady-state results in Figure 3 are quite similar to those in Figure 2. Thus, the addition of a "complete" gas-grain reaction network does not change significantly the abundance of surface H_2 as a function of density.

[2] Values used in this study come from Graedel et al. (1982), Wakelam & Herbst (2008), and Jenkins (2009).

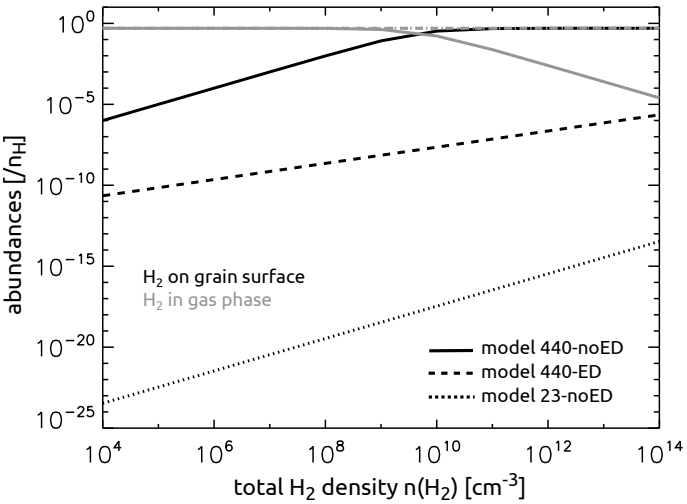

Fig. 3. H_2 fractional abundance in the gas phase (gray) and on the dust grain surface (black) relative to n_H as a function of total H_2 density for the three models 440-noED (solid line), 23-noED (dotted line), and 440-ED (dashed line). The dotted and dashed gray lines, which blend into one another, are horizontal and lie atop the figure.

We note specifically the results for a standard cold dense cloud with the inclusion of encounter desorption (model 440-ED): the H_2 fractional surface abundance lies between 10^{-11} and 10^{-10} for a standard cold dense cloud, which represent respectively $\sim$ 10 and $\sim$ 100 molecules on the surface of a dust grain.

The use of encounter desorption, as seen in Figures 2 and 3, clearly reduces the amount of surface H_2 at all densities chosen. These lowered abundances, however, are still significantly higher than what can be obtained if we assume that H_2 cannot stick to grains at all, and that all of the molecular hydrogen on grains comes directly from its formation from two H atoms that have accreted onto the surface. Thus the implementation of encounter desorption does not lead to the same situation as the assumption of no sticking of H_2, at least at the densities studied.

The amount of surface hydrogen is likely to affect the chemistry and abundance of other species, both gaseous and solid-state, especially at densities significantly higher than those pertaining to cold dense clouds. Some of the effect derives from radical-H_2 surface reactions that can occur even at low temperatures on the surface via tunneling (Hasegawa & Herbst 1993a). In the following section, we discuss the impact of H_2 grain coverage on the abundances of other species for sources at 10 K and a range of densities.

5. Discussion

We computed the time-dependent chemical evolution under the same range of physical conditions as used previously and with the models listed in Table 1. Although the higher density models are not relevant to dense cores, they can be relevant to the dense midplane of protoplanetary disks and to centers of prestellar isothermally collapsing cores. Moreover, hydrodynamic calculations can lead to temporary high densities and low temperatures.

We start with a comparison of the gas-phase abundances measured for the cold cores TMC-1CP and L134N and the gas-phase results of the three models using a comparison parameter D between modeling results and observational constraints, given

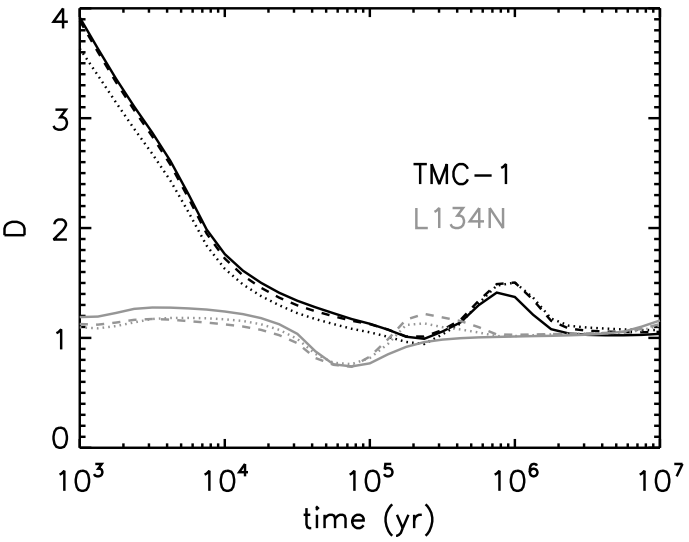

Fig. 4. Parameter D as a function of time for TMC-1 (black) and L134N (gray), using a total hydrogen density of 2×10^4 and 2×10^5 cm^{-3} respectively, for the three models: 440-noED (solid line), 23-noED (dotted line), and 440-ED (dashed line).

by the equation

$$D(t) = \frac{1}{N} \sum_j \left| \log\left(X_j^{mod}(t)\right) - \log\left(X_j^{obs}\right) \right|. \quad (5)$$

Here, X_j^{obs} is the observed abundance of species j, $X_j^{mod}(t)$ is the computed abundance of species j at time t, and N is the number of observed species in the cloud. The smaller the value of D, the closer the agreement. We used the observed abundances listed in Agúndez & Wakelam (2013)[3]. There is little difference in the results for $D(t)$ using the three models at densities of 2×10^4 and 2×10^5 cm^{-3}, as shown in Figure 4.

For individual species, however, the three models can yield different results, even in the gas-phase. For an example, let us consider the major species water, CO, and methane, and the atomic carbon. Panels A and B of Figure 5 show the abundances of water, carbon monoxide, and methane both on the grain surface and in the gas phase, as a function of total H_2 density, for the three models at 10^6 yrs, a time relevant for protoplanetary disks and older cold cores. Grain surface abundances of these three species are sensitive to the model used, but in the gas phase, only water is strongly affected by the choice of model. However, while the grain surface abundances of these species vary by a maximum factor of three, the gas phase water abundance is decreased by three orders of magnitude at 10^9 cm^{-3} going from model 440-ED to 440-noED, which corresponds to an increase in sH_2, where the "s" stands for "grain surface". The depletion in gaseous H_2 leads to a depletion of precursors to gaseous water and to an increase of sH_2, which consumes sOH so that the production of gas phase water through reactive desorption with sH is lessened. The abundance of solid atomic carbon, seen in Panel C, also depends strongly on the sH_2 abundance. In model 440-noED, where sH_2 is highest, the abundance of sC is lowest due to its destruction via reaction with sH_2.

Depending on the density and the time considered, a general behavior can be seen for the majority of grain surface species, based upon the surface H_2 abundance (see Figure 3). At the lowest densities, model 440-noED and 440-ED present the same results, while the results of model 23-noED are different. At the highest densities, model 440-noED shows different results from the two others, which are quite similar. Thus the encounter desorption model starts out similarly to the model with a desorption energy for H_2 of 440 K and ends up, with increasing density, similar to the model with a lower desorption energy of 23 K. This relation can be understood by the following argument. At the lowest densities, H_2 does not adsorb very much, so encounter desorption is not very efficient since sH_2 lies mainly on top of the water substrate. At the highest densities, H_2 builds hundreds or even thousands of monolayers if we consider a fixed desorption energy of H_2 of 440 K, while encounter desorption becomes quite efficient in these conditions. We can then discriminate among three different regimes. The first one occurs when almost no H_2 at all is present on the grain surface (model 23-noED at the lowest densities), the second one when some H_2 is present at an "intermediate level" (models 440-ED and 440-noED at the lowest densities, and models 440-ED and 23-noED at the highest densities), and a third one when H_2 is very abundant on the grain surface and depletion of H_2 from the gas phase is large (model 440-noED at the highest densities).

Figure 6 shows these different regimes and the transition from one regime to another one for sCO_2. At 2×10^5 yr and 10^4 cm^{-3}, models 440-noED and 440-ED give close results while model 23-noED gives $\sim$ 4 times more sCO_2. Between 10^5 and 10^{11} cm^{-3}, each model gives different results, during this transitional range. At the highest densities, models 440-ED and 23-noED give same result and the third model gives slightly different results. However, these transitions are not only density dependent, but also somewhat time dependent. At 10^7 yrs and 10^4 cm^{-3}, all models give similar results, while outside this density range, models 440-ED and 23-noED give similar results and model 440-noED gives different ones.

5.1. Sticking probability

We assume a sticking probability S equal to unity, which means that each collision between a gas phase species and a grain results in an adsorption. In reality, this probability depends on numerous parameters such as the gas and grain temperature (e.g. Fillion et al. 2011) as well as the composition and the structure of the grain surface (e.g. Hollenbach & Salpeter 1970; Buch & Zhang 1991; Masuda et al. 1998). Recently, Acharyya (2014) has experimentally studied the sticking coefficient of H_2 on an olivine substrate, and estimated a lower limit from 0.25 to 0.82 for temperatures between 7 K and 14 K. Our initial assumption may have some impact on our results, so we tested the sensitivity of the rate equation model to this coefficient using a value equal to 0.5.

With $S = 0.5$, the abundance of sH_2 is decreased while the abundance of gas phase H_2 is increased, both by a factor $\sim$ 10 maximum. In the 440-noED model, all hydrogen is located on the grain surface as the densities approaches 10^{12} cm^{-3}, a roughly ten times higher value than with $S = 1$. This result

[3] Values used in this study come from Matthews et al. (1985), Matthews et al. (1987), Minh et al. (1989), Schilke et al. (1991), Kawaguchi et al. (1992a), Kawaguchi et al. (1992b), Ohishi et al. (1992), Gerin et al. (1993), McGonagle et al. (1994), Ohishi et al. (1994), Pratap et al. (1997), Langer et al. (1997), Guelin et al. (1998), Ohishi & Kaifu (1998), Takano et al. (1998), Bell et al. (1999), Snell et al. (2000), Dickens et al. (2000), Turner et al. (2000), Pagani et al. (2003), Remijan et al. (2006), Snyder et al. (2006), Akyilmaz et al. (2007), Brünken et al. (2007), Agúndez et al. (2008), Marcelino et al. (2009), Gupta et al. (2009), and Cernicharo et al. (2011).

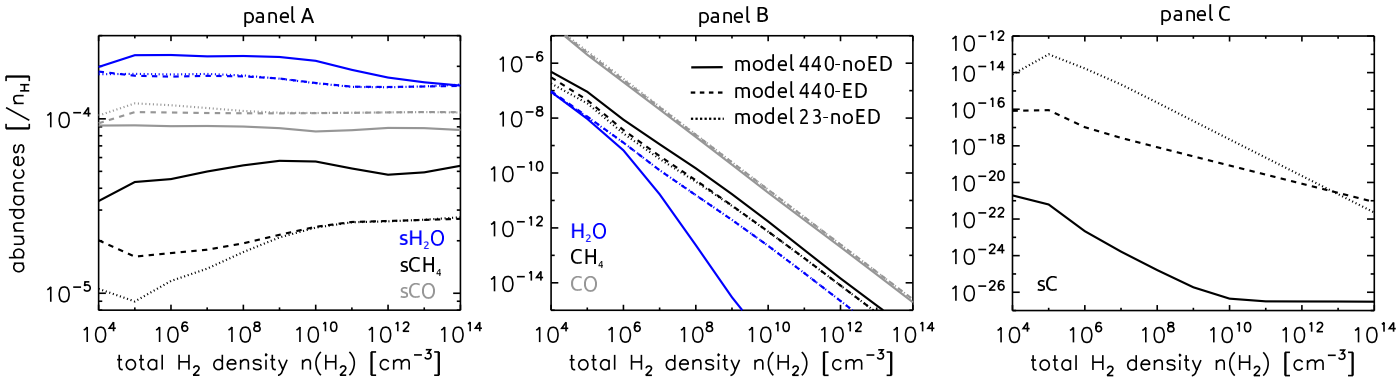

Fig. 5. H_2O (blue), CO (gray), and CH_4 (black) abundances at 10^6 yr on a grain surface (panel A) and in the gas phase (panel B) plotted against total H_2 density for the three models 440-noED (solid line), 23-noED (dotted line), and 440-ED (dashed line). Panel C contains the atomic carbon abundance on a grain surface at the same time and the same models.

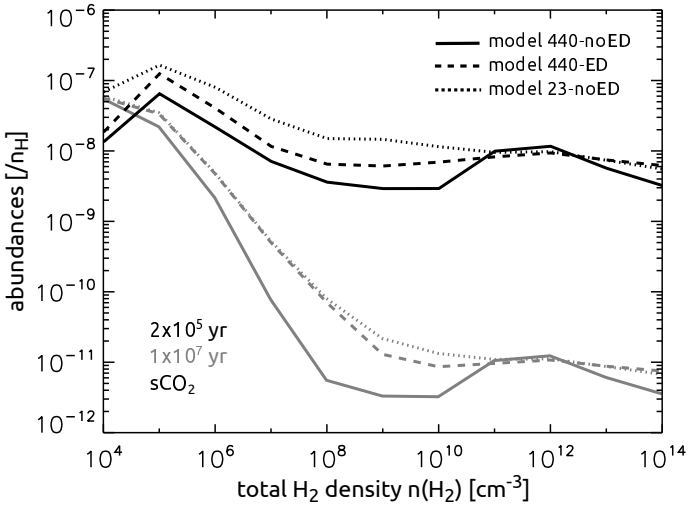

Fig. 6. CO_2 abundance on the grain surface at 2×10^5 yrs (black) and 10^7 yrs (gray) for the three models 440-noED (solid line), 23-noED (dotted line), and 440-ED (dashed line).

comes obviously from the lower adsorption rate of gas phase H_2 to the grain surface. The sensitivity of other molecules to the value of S also comes from whether they are formed in the gas or on grains. Molecules such sH_2O and sCH_4 are efficiently produced on the grain surface, so a decrease in the adsorption rate normally implies a decrease of the abundance of the reactants that will produce these molecules. However, water is also formed in the gas phase , so its sensitivity to S is lower than for methane which is essentially formed on the grain surface; the abundance of water is decreased by a factor of two at most while the factor can be as high as ten for methane. The abundance of sCO is modified by less than a factor two. This small effect stems from two opposing processes: the adsorption rate of CO is lower when S is reduced to 0.5, but the surface reaction rates involving sCO are also lower.

While the abundance for a given molecule can be different when the sticking probability is reduced from 1.0 to 0.5, the relative results of the three models 440-ED, 440-noED, and 23-noED exhibit the same pattern whatever the value of the coefficient is. For example, the abundance of sC is still much lower in the case of the 440-noED model than the other two models, while the gas phase abundances of CO, CH_4, and H_2O are still not dependent on the model, except for water at densities higher than 10^7 cm^{-3} for the 440-noED model as shown in panel B of figure 5. As a consequence, we conclude that the value of the sticking coefficient does not impact the relative efficiency of encounter desorption significantly.

5.2. Initial abundances

We typically start with all hydrogen in its molecular form. To test the sensitivity of encounter desorption to this assumption, we also performed some simulations with all hydrogen initially in its pure atomic form. The results for the three models 440-ED, 440-noED, and 23-noED are presented in Figure 7, at the same time (10^6 yr) and for the same species as in Figure 5 to allow for an easy comparison. The abundance profiles of surface atomic carbon and gas phase water, carbon monoxide, and methane are similar to our previous simulation. Due to the high density, adsorption of atomic hydrogen is efficient, and H_2 is formed quickly on the grain surface. Grain surface H_2 needs about 1 yr or less depending on the density to reach steady state, and gas phase H_2 needs about 10^6 and 10^1 yrs to reach steady state at a total proton density of 2×10^4 and 2×10^8 cm^{-3} respectively. The case of the main ices is however slightly different. They are formed faster, since hydrogenation by s-H is more efficient. Besides, surface atomic carbon is primarily converted into methane rather than carbon monoxide. For these ices, the abundance of sH_2 seems less critical than for our previous simulations and as a consequence differences between the results of models 440-ED, 440-noED, and 23-noED are reduced. In conclusion, our results are still sensitive to encounter desorption at 10^6 yr using atomic hydrogen as an initial condition, depending on the considered species.

5.3. Motion through quantum tunneling

We typically assume thermal diffusion. We also studied the sensitivity of our three models 440-ED, 440-noED, and 23-noED to the motion of H_2 through quantum tunneling. The abundances of H_2 in the gas phase and on the grain surface are not changed for the two models 440-noED and 23-noED using this new assumption, at all times and densities. For the third model, abundance of s-H_2 is however reduced by about three orders of magnitude compared to the same model without tunneling, at all times and densities. Since motion through quantum tunneling is faster than thermal diffusion at 10 K, encounter desorption happens more frequently and reduces the surface abundance of H_2. As a consequence for the molecules studied in this paper, the results of

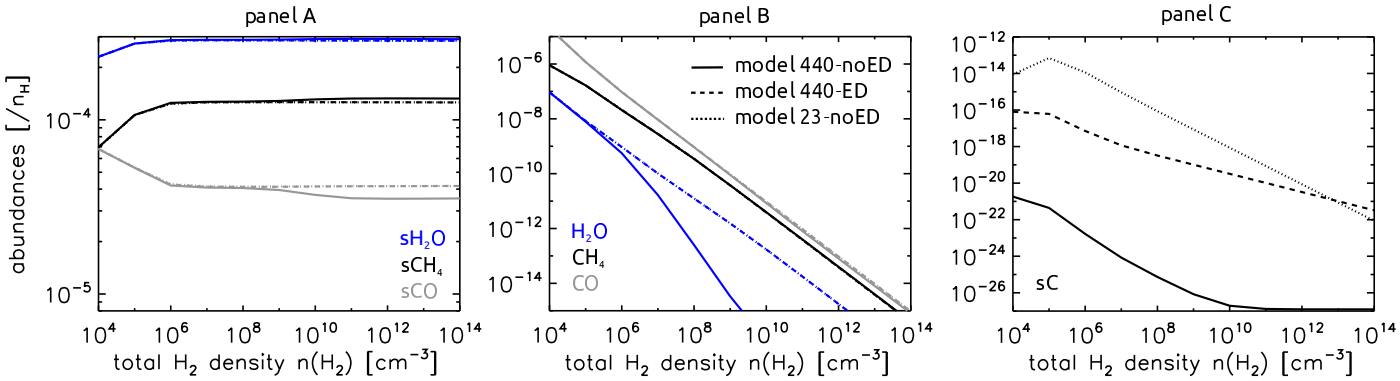

Fig. 7. Same as Figure 5. Hydrogen is initially in atomic rather than molecular form.

440-ED model are closer to those of the 23-noED model. Depending on the density and the time however, results of these two models can still be quite different.

6. Conclusion

We have developed a new approach to prevent a huge accumulation of H_2 on interstellar grain surfaces at low temperatures and high densities, which should not occur because the desorption energy of H_2 on an H_2 substrate is much lower than on a water substrate. This method, which is to be used in gas-grain rate-equation simulations, is based on the facile desorption of molecular hydrogen when it encounters a molecule of an H_2 substrate. We have named this process "encounter desorption".

In order to test our approach, we first used a very simple system including the encounter desorption process to calculate the surface abundance of H_2 molecules as a function of density at a temperature of 10 K. We then compared our result with an analogous but more exact result obtained using a microscopic Monte Carlo stochastic method. A comparison between the steady-state results of the rate-equation model with encounter desorption and the Monte-Carlo approach gives very good agreement for gas densities from 10^4 to 10^{12} cm^{-3}. Above 10^{12} cm^{-3}, the rate-equation model slightly overestimates the H_2 grain surface abundance, by a factor of up to 4. We then used a complete gas-grain network with the Nautilus model to which encounter desorption was added and repeated the steady-state rate-equation calculation of the surface abundance of H_2 vs density, obtaining very similar results to both the simple rate-equation and Monte Carlo treatments. We thus conclude that the approach is a reasonable one, although the mathematics do not distinguish between the surface layer of an ice mantle and the inner layers.

We also studied the impact of different H_2 surface abundances on the abundance of other species, using two models with a fixed desorption energy of H_2 (23 K and 440 K) and one model with the encounter desorption mechanism. The sensitivity of the results of these models is relatively complex, and depends on the considered chemical species, the density of the medium, and the time. Nevertheless, the calculated abundances can often be divided into three regions depending upon whether the H_2 surface coverage is low, intermediate, or high. Reducing the sticking coefficient for adsorption from unity to 0.5 does not change these results.

We tested the sensitivity of our models to a different initial condition – hydrogen initially in atomic form instead of molecular – and to the motion of H_2 via quantum tunneling instead of only thermal diffusion. These assumptions may change the abundances of some species depending on the density and the time, but our simulations are generally still sensitive to the encounter desorption mechanism, and the results mentioned in the previous paragraph often still hold.

Our results highlight the need to incorporate in rate-equation models a way to more correctly model H_2 coverage at low temperature and high density. This need becomes even more pressing when physical conditions present huge variations, such as during the collapse of a prestellar core to form a protostar surrounded by a disk. In this scenario, matter transits through variations of both density and temperature, which lead to potentially large variations of H_2 coverage, some quite unphysical such as the limit in which all H_2 lies on interstellar grain mantles. The encounter desorption method keeps the amount of H_2 at physically reasonable values by using both the desorption energy of H_2 on a water ice mantle and on a mantle with some H_2 on its surface. The approach computes the rate of encounter desorption "on the fly", i.e., as a function of time and H_2 coverage, and therefore is well designed for a scenario in which the physical conditions are rapidly changing. In addition, it is relatively easy to implement, and is not significantly CPU time consuming. Although H_2 is the most abundant molecule in the interstellar medium, a possible extension to this work would be to consider encounter desorption for other weakly bound atoms and molecules.

Acknowledgements. U. Hincelin thanks G. Hassel for help in adding photodesorption processes to the chemical code, and K. Acharyya and K. Furuya for useful discussions. We thank the anonymous referee for suggestions that helped us to improve our paper. E. Herbst acknowledges the support of the National Science Foundation (US) for his astrochemistry program, and support from the NASA Exobiology and Evolutionary Biology program through a subcontract from Rensselaer Polytechnic Institute. Some kinetic data we used have been downloaded from the online database KIDA (KInetic Database for Astrochemistry, `http://kida.obs.u-bordeaux1.fr`, Wakelam et al. (2012)).

References

Acharyya, K. 2014, MNRAS, 443, 1301
Agúndez, M., & Wakelam, V. 2013, Chemical Reviews, 113, 8710
Agúndez, M., Cernicharo, J., Guélin, M., et al. 2008, A&A, 478, L19
Akyilmaz, M., Flower, D. R., Hily-Blant, P., Pineau Des Forêts, G., & Walmsley, C. M. 2007, A&A, 462, 221
Bell, M. B., Feldman, P. A., Watson, J. K. G., et al. 1999, ApJ, 518, 740
Brünken, S., Gupta, H., Gottlieb, C. A., McCarthy, M. C., & Thaddeus, P. 2007, ApJ, 664, L43
Buch, V., & Zhang, Q. 1991, ApJ, 379, 647
Caselli, P., Hasegawa, T. I., & Herbst, E. 1998, ApJ, 495, 309
Cazaux, S., Cobut, V., Marseille, M., Spaans, M., & Caselli, P. 2010, A&A, 522, A74
Cernicharo, J., Spielfiedel, A., Balança, C., et al. 2011, A&A, 531, A103
Chang, Q., & Herbst, E. 2012, ApJ, 759, 147
Chang, Q., & Herbst, E. 2014, ApJ, 787, 135

Chang, Q., Cuppen, H. M., & Herbst, E. 2005, A&A, 434, 599
Chang, Q., Cuppen, H. M., & Herbst, E. 2007, A&A, 469, 973
Cuppen, H. M., & Garrod, R. T. 2011, A&A, 529, A151
Cuppen, H. M., & Herbst, E. 2005, MNRAS, 361, 565
Cuppen, H. M., & Herbst, E. 2007, ApJ, 668, 294
Cuppen, H. M., van Dishoeck, E. F., Herbst, E., & Tielens, A. G. G. M. 2009, A&A, 508, 275
Dickens, J. E., Irvine, W. M., Snell, R. L., et al. 2000, ApJ, 542, 870
Fillion, J. H., Dulieu, F., Romanzin, C., & Cazaux, S. 2011, European Physical Journal Web of Conferences, 18, 3002
Furuya, K., Aikawa, Y., Tomida, K., et al. 2012, ApJ, 758, 86
Garrod, R. T., & Herbst, E. 2006, A&A, 457, 927
Garrod, R. T., & Pauly, T. 2011, ApJ, 735, 15
Garrod, R. T., Weaver, S. L. W., & Herbst, E. 2008, ApJ, 682, 283
Gerin, M., Viala, Y., & Casoli, F. 1993, A&A, 268, 212
Graedel, T. E., Langer, W. D., & Frerking, M. A. 1982, ApJS, 48, 321
Guelin, M., Neininger, N., & Cernicharo, J. 1998, A&A, 335, L1
Gupta, H., Gottlieb, C. A., McCarthy, M. C., & Thaddeus, P. 2009, ApJ, 691, 1494
Hasegawa, T. I., & Herbst, E. 1993a, MNRAS, 261, 83
Hasegawa, T. I., & Herbst, E. 1993b, MNRAS, 263, 589
Hasegawa, T. I., Herbst, E., & Leung, C. M. 1992, ApJS, 82, 167
Hassel, G. E., Herbst, E., & Garrod, R. T. 2008, ApJ, 681, 1385
Hassel, G. E., Herbst, E., & Bergin, E. A. 2010, A&A, 515, A66
Herbst, E., & Klemperer, W. 1973, ApJ, 185, 505
Herbst, E., & Shematovich, V. I. 2003, Ap&SS, 285, 725
Hersant, F., Wakelam, V., Dutrey, A., Guilloteau, S., & Herbst, E. 2009, A&A, 493, L49
Hincelin, U. 2012, Ph.D. Thesis
Hincelin, U., Wakelam, V., Hersant, F., et al. 2011, A&A, 530, A61
Hincelin, U., Wakelam, V., Commerçon, B., Hersant, F., & Guilloteau, S. 2013, ApJ, 775, 44
Hollenbach, D., & Salpeter, E. E. 1970, J. Chem. Phys., 53, 79
Iqbal, W., Acharyya, K., & Herbst, E. 2012, ApJ, 751, 58
Jenkins, E. B. 2009, ApJ, 700, 1299
Kawaguchi, K., Ohishi, M., Ishikawa, S.-I., & Kaifu, N. 1992a, ApJ, 386, L51
Kawaguchi, K., Takano, S., Ohishi, M., et al. 1992b, ApJ, 396, L49
Langer, W. D., Velusamy, T., Kuiper, T. B. H., et al. 1997, ApJ, 480, L63
Leger, A., Jura, M., & Omont, A. 1985, A&A, 144, 147
Lipshtat, A., & Biham, O. 2003, A&A, 400, 585
Marcelino, N., Cernicharo, J., Tercero, B., & Roueff, E. 2009, ApJ, 690, L27
Masuda, K., Takahashi, J., & Mukai, T. 1998, A&A, 330, 773
Matthews, H. E., Friberg, P., & Irvine, W. M. 1985, ApJ, 290, 609
Matthews, H. E., MacLeod, J. M., Broten, N. W., Madden, S. C., & Friberg, P. 1987, ApJ, 315, 646
McGonagle, D., Irvine, W. M., & Ohishi, M. 1994, ApJ, 422, 621
Minh, Y. C., Irvine, W. M., & Ziurys, L. M. 1989, ApJ, 345, L63
Morata, O., & Hasegawa, T. I. 2013, MNRAS, 429, 3578
Öberg, K. I., Fuchs, G. W., Awad, Z., et al. 2007, ApJ, 662, L23
Öberg, K. I., Garrod, R. T., van Dishoeck, E. F., & Linnartz, H. 2009a, A&A, 504, 891
Öberg, K. I., Linnartz, H., Visser, R., & van Dishoeck, E. F. 2009b, ApJ, 693, 1209
Öberg, K. I., van Dishoeck, E. F., & Linnartz, H. 2009c, A&A, 496, 281
Ohishi, M., & Kaifu, N. 1998, Faraday Discussions, 109, 205
Ohishi, M., Irvine, W. M., & Kaifu, N. 1992, Astrochemistry of Cosmic Phenomena, 150, 171
Ohishi, M., McGonagle, D., Irvine, W. M., Yamamoto, S., & Saito, S. 1994, ApJ, 427, L51
Pagani, L., Olofsson, A. O. H., Bergman, P., et al. 2003, A&A, 402, L77
Pratap, P., Dickens, J. E., Snell, R. L., et al. 1997, ApJ, 486, 862
Remijan, A. J., Hollis, J. M., Snyder, L. E., Jewell, P. R., & Lovas, F. J. 2006, ApJ, 643, L37
Ruffle, D. P., & Herbst, E. 2000, MNRAS, 319, 837
Semenov, D., Hersant, F., Wakelam, V., et al. 2010, A&A, 522, A42
Schilke, P., Walmsley, C. M., Henkel, C., & Millar, T. J. 1991, A&A, 247, 487
Snell, R. L., Howe, J. E., Ashby, M. L. N., et al. 2000, ApJ, 539, L101
Snyder, L. E., Hollis, J. M., Jewell, P. R., Lovas, F. J., & Remijan, A. 2006, ApJ, 647, 412
Stantcheva, T., & Herbst, E. 2004, A&A, 423, 241
Takano, S., Masuda, A., Hirahara, Y., et al. 1998, A&A, 329, 1156
Taquet, V., Ceccarelli, C., & Kahane, C. 2012, A&A, 538, A42
Tielens, A. G. G. M., & Allamandola, L. J. 1987, Interstellar Processes, 134, 397
Tielens, A. G. G. M., & Charnley, S. B. 1997, Origins of Life and Evolution of the Biosphere, 27, 23
Tielens, A. G. G. M., & Hagen, W. 1982, A&A, 114, 245
Turner, B. E., Herbst, E., & Terzieva, R. 2000, ApJS, 126, 427
Viti, S., Collings, M. P., Dever, J. W., McCoustra, M. R. S., & Williams, D. A. 2004, MNRAS, 354, 1141
Wakelam, V., & Herbst, E. 2008, ApJ, 680, 371
Wakelam, V., Herbst, E., Loison, J.-C., et al. 2012, ApJS, 199, 21
Watson, W. D. 1976, Reviews of Modern Physics, 48, 513
Wolff, A., Lohmar, I., Krug, J., Frank, Y., & Biham, O. 2010, Phys. Rev. E, 81, 061109
Whittet, D. C. B., Gerakines, P. A., Tielens, A. G. G. M., et al. 1998, ApJ, 498, L159